Journal of Fundamental and Applied Research **Vol. 5**, Issue 4 (2025) **20250022**

Received: 11 August 2025 / Accepted: 03 November 2025
Published online: 04 November 2025
© 2025 The Author(s)

The magnetic phase diagram of cuprates from a two-scale polaron model

Orifjon Ganiev[1, 2, *]

[1]*Institute of Nuclear Physics, AS RUz, 100214 Tashkent, Uzbekistan*
[2]*National University of Uzbekistan, 100174 Tashkent, Uzbekistan*

Abstract. We present a theoretical framework for the magnetic field-hole doping ($H-p$) phase diagram of cuprate superconductors. The theory is based on a two-scale polaronic model that distinguishes the high-energy formation of polarons, which sets the pseudogap energy scale Δ_p, from the low-energy phase coherence of polaron pairs, which determines the superconducting transition temperature T_c. We show that these two distinct energy scales generate two fundamental, independent length scales that govern the response of the system to an applied magnetic field. Our framework quantitatively reproduces the characteristic dome of the upper critical field, $H_{c2}(p)$, as a direct consequence of the doping-dependent phase coherence. Furthermore, we identify a significantly higher magnetic field, $H^*(p)$, corresponding to the breaking of pre-formed pairs. This upper field terminates at a pseudogap quantum critical point (QCP), where Coulomb repulsion ultimately unbinds the pairs. The theoretical predictions for both the superconducting coherence length $\xi_c(p)$ and the upper critical field $H_{c2}(p)$ show excellent quantitative agreement with experimental thermodynamic data for the $La_{2-x}Sr_xCuO_4$ system, without the need for any free fitting parameters.

Key words: magnetic field-doping, polaron, QCP, superconductivity, superfluid.

I. INTRODUCTION

Despite decades of intensive research, the mechanism underlying high-temperature superconductivity in the cuprates remains one of the most significant and debated problems in condensed matter physics [1, 2]. A central and enigmatic feature of these materials is the pseudogap (PG) phase, which coexists and competes with superconductivity in the underdoped region of the phase diagram [3]. While the temperature-doping ($T-p$) phase diagram is well-documented, the magnetic field-doping ($H-p$) plane offers crucial complementary insights into the fundamental energy scales governing the system.

Experimental investigations of the $H-p$ phase diagram reveal a characteristic dome-shaped upper critical field, $H_{c2}(p)$, which peaks at a similar optimal doping level as the superconducting transition temperature, T_c [4, 5]. Moreover, quasiparticle tunneling experiments, such as scanning tunneling spectroscopy (STS), have shown that a gap-like feature persists not only above T_c in the PG regime but also at low temperatures within the cores of magnetic vortices where superconductivity is locally suppressed [2, 6]. This strongly suggests that the energy gap associated with pair formation is distinct from the energy scale for long-range phase coherence, which underpins macroscopic superconductivity.

This two-scale paradigm posits a scenario of pre-formed pairs: charge carriers bind into pairs at a high temperature or energy scale (related to the pseudogap), but these pairs only establish long-range phase coherence to form a superconducting condensate at a lower temperature, T_c [7]. This behavior is characteristic of a system in the BCS-BEC crossover regime. A compelling physical origin for this can be attributed to the formation of polarons – quasiparticles "dressed" by a cloud of lattice vibrations (phonons) due to strong electron-phonon coupling, a known feature of cuprates [8, 9]. The strong binding of these polarons can naturally lead to pre-formed pairs, while their collective coherence gives rise to superconductivity [10].

In this paper, we develop a comprehensive theoretical model based on this two-scale polaronic picture. We demonstrate that the interplay between two distinct, doping-dependent length scales – one related to the size of the pre-formed pair and the other to the superconducting coherence length – is sufficient to quantitatively explain the entire $H-p$ phase diagram. Our model not only naturally reproduces the H_{c2} dome but also provides a physical mechanism for the pseudogap QCP. Importantly, our results show excellent quantitative agreement with bulk thermodynamic measurements on $La_{2-x}Sr_xCuO_4$ (LSCO), a canonical cuprate superconductor.

* Corresponding author: oganiev@yahoo.com

II. THEORETICAL MODEL

A. The Polaronic Pseudogap and the QCP

We propose that the pseudogap in cuprates is a direct manifestation of the formation of tightly bound polaronic pairs. The net energy required to break such a pair, which we identify as the pseudogap energy Δ_p, is determined by a competition between the intrinsic polaron binding energy, E_p, and the mean-field Coulomb repulsion energy between them, E_c. This can be expressed as [10, 11]:

$$\Delta_p(p) = E_p - E_c(p). \tag{1}$$

The Coulomb repulsion energy E_c is inversely proportional to the mean distance between polarons a_p, i.e., $E_c = e^2/(\epsilon_0 a_p)$, where ϵ_0 is the static dielectric constant. As the hole doping p increases, the density of polarons rises, causing a_p to decrease and, consequently, E_c to rise. This doping-dependent competition provides a natural explanation for the closing of the pseudogap at a critical doping level. The PG phase terminates at a pseudogap quantum critical point (QCP), $p = p_c$, where the repulsion completely overcomes the binding energy, such that $\Delta_p(p_c) = 0$. This occurs when $E_c(p_c) = E_p$. For doping levels beyond p_c, stable polaron pairs are no longer energetically favorable, and the system transitions into a more conventional metallic state, consistent with experimental findings [12].

B. *d*-wave Superconductivity

Within our model, superconductivity arises when the pre-formed polaronic pairs establish long-range phase coherence. We describe the superconducting state with a momentum-dependent, $d_{x^2-y^2}$-wave gap, $\Delta_{\mathbf{k}} = \Delta_d \cos(2\theta)$. The maximum gap amplitude, $\Delta_d(T, p)$, is determined by solving the self-consistent gap equation for an interacting polaronic Fermi gas:

$$1 = \lambda_d \int_0^{\epsilon_A} d\epsilon \int_0^{2\pi} \frac{d\theta}{2\pi} \cos^2(2\theta) \frac{1}{E_{\mathbf{k}}} \tanh\left(\frac{E_{\mathbf{k}}}{2k_B T}\right), \tag{2}$$

where $E_{\mathbf{k}} = \sqrt{\epsilon^2 + \Delta_d^2 \cos^2(2\theta)}$, λ_d is the dimensionless d-wave pairing strength, and ϵ_A is a physically motivated energy cutoff determined by the polaron structure ($\epsilon_A = E_p + \hbar\omega_{LO}$). The model is grounded in experimental reality by linking it to the well-established empirical form of the superconducting dome. We determine the doping dependence of the pairing strength $\lambda_d(p)$ by requiring that Eq. (2), in the limit $\Delta_d \to 0$, reproduces the known parabolic dependence of T_c on doping for cuprates: $T_c(p) = T_{c,\max}[1\text{–}82.6(p\text{–}0.16)^2]$ [1, 13].

C. From Energy Scales to Critical Fields

The two distinct energy scales, the pseudogap Δ_p and the superconducting phase coherence energy $\beta_c \propto \Delta_d$, give rise to two fundamentally different length scales. The first is the size of an individual, pre-formed polaron pair, ξ^*, determined by its binding energy:

$$\xi^*(p) = \frac{\hbar}{\sqrt{2m_p \Delta_p(p)}}, \tag{3}$$

where m_p is the effective mass of a single polaron. The second is the Ginzburg-Landau superconducting coherence length, ξ_c, which represents the average size of a polaronic Cooper pair within the condensate and is set by the phase coherence energy β_c:

$$\xi_c(p) = \frac{\hbar}{\sqrt{2m_{cp} \beta_c(p)}}, \tag{4}$$

where m_{cp} is the effective mass of a coherent Cooper pair.

These two length scales, in turn, define two distinct characteristic magnetic fields. Superconductivity is thermodynamically suppressed when magnetic flux vortices, each of size $\sim \xi_c$, are forced to overlap. This condition defines the upper critical field, H_{c2}:

$$H_{c2}(p) = \frac{\Phi_0}{2\pi \xi_c(p)^2} \propto \beta_c(p), \tag{5}$$

 Copyright © 2025

where Φ_0 is the magnetic flux quantum. Following the same logic, we define a much larger pseudogap-breaking field, H^*, representing the immense field required to overcome the intra-pair binding and destroy the pre-formed pair itself:

$$H^*(p) = \frac{\Phi_0}{2\pi\xi^*(p)^2} \propto \Delta_p(p). \tag{6}$$

The clear hierarchy of energy scales, $\Delta_p > \beta_c$, in the underdoped regime implies a corresponding hierarchy of length scales, $\xi^* < \xi_c$, and magnetic fields, $H^* > H_{c2}$.

III. RESULTS AND DISCUSSION

A. Magnetic Phase Diagram at T = 0

Solving our model equations yields the full magnetic field-doping phase diagram at $T = 0$, as shown in Fig. 1. The solid line represents the upper critical field $H_{c2}(p)$, calculated from the phase coherence energy via Eq. (5). Its shape is a direct consequence of the doping dependence of the superfluid stiffness, which is weakest at the edges of the superconducting dome (large ξ_c, low H_{c2}) and strongest near optimal doping (small ξ_c, high H_{c2}). This result demonstrates that the famous H_{c2} dome is governed not by the raw pairing strength but by the evolution of collective phase coherence.

The dashed line represents the pseudogap-breaking field $H^*(p)$, derived from the net pairing energy Δ_p via Eq. (6). Following the behavior of Δ_p, H^* is extremely large at low doping (> 600 T) and decreases sharply, terminating at the QCP ($p_c \approx 0.20$), where the field required to break the pairs vanishes. The region between H_{c2} and H^* defines a field-induced pseudogap phase, where long-range phase coherence is destroyed by the magnetic field but pre-formed, incoherent pairs survive.

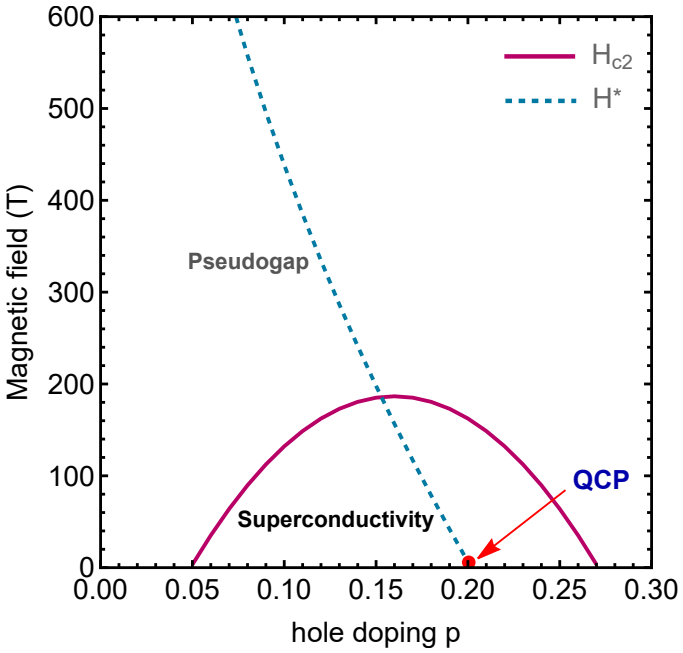


FIG. 1: The calculated magnetic field vs. hole doping phase diagram at $T = 0$. The upper critical field H_{c2} (solid line) forms the characteristic dome marking the boundary of phase-coherent superconductivity. The pseudogap characteristic field H^* (dashed line), which marks the destruction of pre-formed pairs, is much larger and terminates at the pseudogap quantum critical point (QCP) at $p \approx 0.20$.

B. Quantitative Comparison with $La_{2-x}Sr_xCuO_4$

To validate the predictive power of our model, we perform a direct, quantitative comparison with experimental thermodynamic data for the LSCO system. We use the experimental $T_c(p)$ dome for LSCO ($T_{c,\max} = 38$ K) and other known material parameters ($E_p = 0.0541$ eV, $m_{cp} = 4.5m_e$, $m_p = 1.8m_e$) as inputs [5], with no free fitting parameters in the final comparison.

Copyright © 2025

Figure 2(a) compares our calculated superconducting coherence length $\xi_c(p)$ (solid line) with the experimental values derived by Wang and Wen from bulk specific heat measurements [5] (circles). The model accurately reproduces both the quantitative values and the characteristic "U"-shaped trend of the experimental data. This excellent agreement confirms that our model correctly captures the non-monotonic evolution of the superfluid stiffness with doping.

The power of this physical picture is demonstrated in Fig. 2(b). Here, we use the calculated coherence length from Fig. 2(a) to derive the upper critical field $H_{c2}(p)$ via Eq. (5). This is a direct physical prediction, not an independent fit. The resulting theoretical curve (solid line) shows excellent quantitative agreement with the experimentally observed critical field dome. The fact that a single, unified physical model based on polaronic charge carriers can simultaneously account for both the coherence length (superfluid stiffness) and the upper critical field (vortex packing limit) provides compelling evidence for our approach.

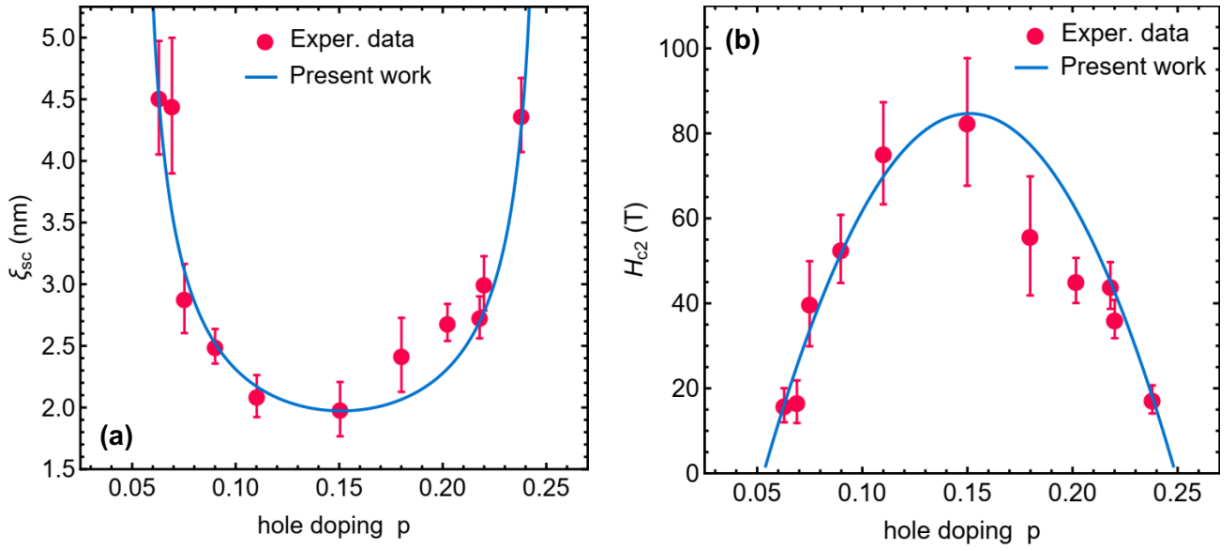


FIG. 2: Comparison of the model with experimental data for $La_{2-x}Sr_xCuO_4$ from Ref. [5] (circles). (a) The calculated superconducting coherence length $\xi_c(p)$ (solid line) accurately reproduces the experimental data. (b) The upper critical field $H_{c2}(p)$, derived directly from the theoretical ξ_c in panel (a), shows excellent quantitative agreement with the experimentally observed critical field dome.

C. The Three-Dimensional $H - p - T$ Phase Boundary

By extending the self-consistent gap equation (Eq. 2) to finite temperatures, we can construct the full three-dimensional $H - p - T$ phase boundary for superconductivity. The temperature-dependent behavior of the coherence length $\xi_c(p, T)$ has crucial implications: for any given doping, ξ_c increases as temperature rises due to the thermal weakening of phase coherence. This, in turn, causes the $H_{c2}(p)$ dome to systematically decrease in height and narrow in width as temperature increases.

Figure 3 synthesizes these results, showing the calculated surface $H_{c2}(p, T)$ which represents the thermodynamic boundary for macroscopic, phase-coherent superconductivity. We present this boundary for two systems: LSCO, using the material-specific parameters benchmarked against experiment, and a generic high-T_c cuprate ($T_{c,\max} = 91$ K) modeled on Bi2212, to demonstrate the general applicability of the model. The volume enclosed by this surface delineates the region in parameter space where superconductivity exists. Cross-sections of this surface reproduce the known 2D phase diagrams: the front-facing profile is the $H_{c2}(p)$ dome at $T = 0$, the base of the dome in the $H = 0$ plane is the $T_c(p)$ dome, and slices at constant doping reveal the $H_{c2}(T)$ curve for a specific composition. This unified surface, emerging directly from our two-length-scale model, provides a complete and physically intuitive picture of the interplay of factors governing superconductivity in the cuprates.

IV. CONCLUSION

We have presented a comprehensive theoretical model that explains the magnetic phase diagram of hole-doped cuprates based on a two-scale polaron picture. The fundamental premise is the distinction between the high energy required for polaron-pair formation (the pseudogap, Δ_p) and the lower energy that governs their long-range phase coherence (related to the superconduct-

Copyright © 2025

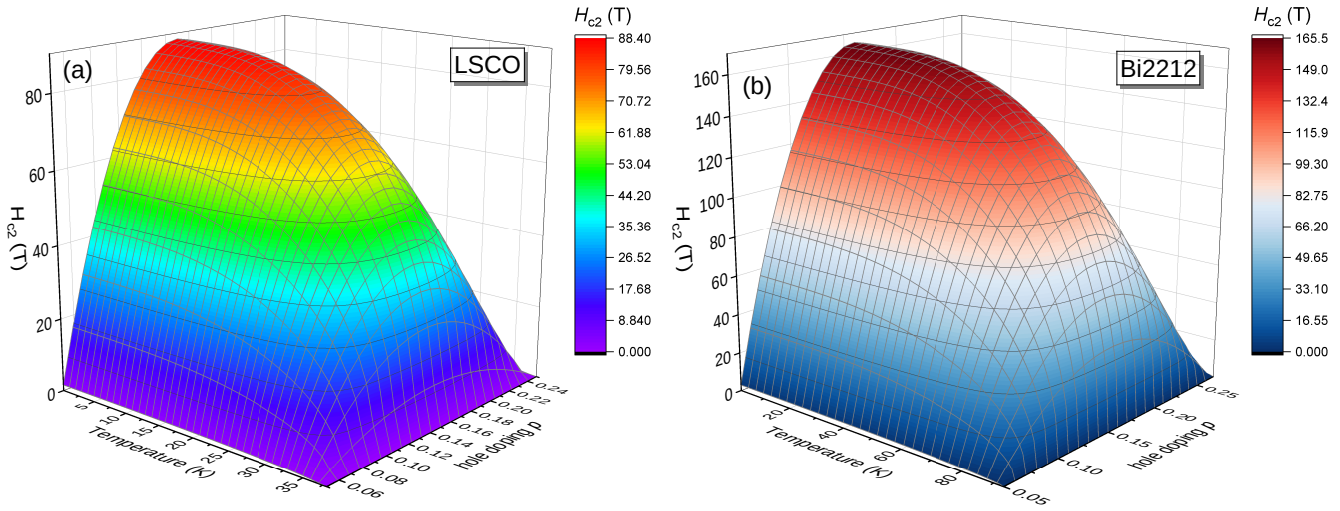


FIG. 3: The three-dimensional $H - p - T$ phase boundary of superconductivity. The surface represents the calculated upper critical field $H_{c2}(p, T)$, which encloses the full thermodynamic region of phase-coherent superconductivity. (a) The calculated boundary for LSCO ($T_{c,\max} = 38$ K), benchmarked against experimental data. (b) The corresponding boundary for a generic high-T_c cuprate modeled on Bi2212 ($T_{c,\max} = 91$ K), demonstrating the general applicability of the model.

ing gap, Δ_d). These two energy scales define two fundamental length scales, ξ^* and ξ_c, which in turn set the critical magnetic fields.

Our primary findings are as follows:

1. The model naturally derives the full $H - p$ phase diagram, explaining the $H_{c2}(p)$ dome as a consequence of the evolution of superfluid stiffness with doping, not raw pairing strength. It also defines a much larger pseudogap-breaking field, $H^*(p)$, which marks the boundary where preformed pairs are destroyed.

2. A physical mechanism for the pseudogap quantum critical point at $p_c \approx 0.20$ is provided, identifying it as the critical doping where mean-field Coulomb repulsion equals the polaron binding energy, making pair formation energetically unfavorable.

3. The predictions of the model for the coherence length $\xi_c(p)$ and the upper critical field $H_{c2}(p)$ are quantitatively confirmed by thermodynamic measurements on LSCO, achieving excellent accuracy without further fitting parameters.

4. By extending the model to finite temperatures, we construct the full three-dimensional $H - p - T$ phase boundary, providing a unified and physically intuitive picture of the superconducting state.

In summary, this work provides a cohesive framework where the complex phase diagram of the cuprates is a direct consequence of the competition between two fundamental polaronic length scales.

REFERENCES

[1] J. Tallon and J. Loram, Physica C: Superconductivity **349**, 53 (2001).
[2] O. Fischer, M. Kugler, I. Maggio-Aprile, C. Berthod, and C. Renner, Rev. Mod. Phys. **79**, 353 (2007).
[3] M. Hashimoto, I. M. Vishik, R.-H. He, T. P. Devereaux, and Z.-X. Shen, Nature Physics **10**, 483 (2014).
[4] G. Grissonnanche, O. Cyr-Choinière, F. Laliberté, S. René de Cotret, A. Juneau-Fecteau, S. Dufour-Beauséjour, M.-È. Delage, D. LeBoeuf, J. Chang, B. J. Ramshaw, D. A. Bonn, W. N. Hardy, R. Liang, S. Adachi, N. E. Hussey, B. Vignolle, C. Proust, M. Sutherland, S. Krämer, J.-H. Park, D. Graf, N. Doiron-Leyraud, and L. Taillefer, Nat. Commun. **5**, 3280 (2014).
[5] Y. Wang and H.-H. Wen, Europhysics Letters **81**, 57007 (2008).
[6] S. H. Pan, E. W. Hudson, A. K. Gupta, K.-W. Ng, H. Eisaki, S. Uchida, and J. C. Davis, Phys. Rev. Lett. **85**, 1536 (2000).
[7] K. Gomes, A. Pasupathy, A. Pushp, S. Ono, Y. Ando, and A. Yazdani, Nature **447**, 569 (2007).
[8] C. Franchini, M. Reticcioli, M. Setvin, and U. Diebold, Nat. Rev. Mater. **6**, 560 (2021).
[9] D. Emin, *Polarons* (Cambridge University Press, Cambridge, 2013).

Copyright © 2025

[10] S. Dzhumanov, Solid State Commun. **115**, 155 (2000).
[11] O. Ganiev, B. Yavidov, S. Kalandarov, I. Rahmonov, and R. Tashkhodjaev, Eur. Phys. J. B **96**, 158 (2023).
[12] N. E. Hussey, Journal of Physics: Condensed Matter **20**, 123201 (2008).
[13] M. Presland, J. Tallon, R. Buckley, R. Liu, and N. Flower, Physica C: Superconductivity **176**, 95 (1991).

Copyright © 2025